JVI Accepted Manuscript Posted Online 18 February 2015
J. Virol. doi:10.1128/JVI.03688-14

Broad-spectrum inhibitors against 3C-like proteases of feline coronaviruses and feline caliciviruses

Yunjeong Kim [a#], Vinay Shivanna [a], Sanjeev Narayanan [a], Allan M. Prior [b*], Sahani Weerasekara [b], Duy H. Hua [b], Anushka C. Galasiti Kankanamalage [c], William C. Groutas [c], and Kyeong-Ok Chang [a]

Department of Diagnostic Medicine and Pathobiology, College of Veterinary Medicine, Kansas State University, Manhattan, Kansas, USA[a]; Department of Chemistry, Kansas State University, Manhattan, Kansas, USA[b]; Department of Chemistry, Wichita State University, Wichita, Kansas, USA[c]

Running Head: Dual inhibitors of feline coronavirus and calicivirus

#Address correspondence to Yunjeong Kim, ykim@vet.k-state.edu.

*Present address: University of the Witwatersrand, Johannesburg, South Africa

Word count for abstract: 250 words

Word count for text: 4479 words

Abstract

Feline infectious peritonitis and virulent, systemic-calicivirus infection are caused by certain types of feline coronaviruses (FCoV) and feline caliciviruses (FCV), respectively, and are important infectious diseases with high fatality rates in members of the Felidae family. While FCoV and FCV belong to two distinct virus families of *Coronaviridae* and *Caliciviridae*, respectively, they share dependence on viral 3C-like protease (3CLpro) for their replication. Since 3CLpro is functionally and structurally conserved among these viruses and essential for viral replication, 3CLpro is considered a potential target for antiviral drug design with broad-spectrum activities against these distinct and highly important viral infections. However, small molecule 3CLpro inhibitors for FCoV and FCV have not been previously identified. In this study, derivatives of peptidyl compounds targeting 3CLpro were synthesized and evaluated against FCoV and FCV. Structures of compounds that show potent dual antiviral activities with a wide margin of safety were identified and discussed. Furthermore, the *in vivo* efficacy of 3CLpro inhibitors was evaluated using a mouse model of coronavirus infection. Intraperitoneal administration of two 3CLpro inhibitors in mice infected with murine hepatitis virus-A59, a hepatotrophic coronavirus, resulted in significant reduction in virus titers and pathological lesions in the liver compared to controls. These results suggest that the series of 3CLpro inhibitors described here may have a potential to be further developed as therapeutic agents for these important viruses in domestic and wild cats. This study provides important insights into the structure and function relationships in 3CLpro for the antiviral drug design with broader antiviral activities.

Importance

Feline infectious peritonitis virus (FIPV) is the leading cause of death in young cats and virulent, systemic calicivirus (vs-FCV) causes a highly fatal disease in cats for which no preventive or therapeutic measure is available. These distinct viruses that belong to different virus families encode structurally and functionally conserved 3C-like protease (3CLpro) which is a potential target for broad-spectrum antiviral drug development. However no studies have previously reported a structural platform for antiviral drug design for these viruses or the efficacy of 3CLpro inhibitors against coronavirus infection in experimental animals. In this study, we explored the structure-activity relationships of the derivatives of 3CLpro inhibitors and identified inhibitors with potent dual activities against these viruses. In addition, the efficacy of the 3CLpro inhibitors was demonstrated in mice infected with a murine coronavirus. Overall, our study provides the first insight into a structural platform for anti-FIPV and FCV drug development.

Introduction

Feline coronaviruses (FCoV) and feline caliciviruses (FCV) are important pathogens of cats and generally cause mild, self-limiting localized infection in the intestinal tract or oral cavity and upper respiratory tract, respectively. However, these viruses can also cause life-threatening systemic illness with high fatality in cats. FCoV associated with fatal disease in cats, feline infectious peritonitis (FIP), causes systemic pyogranulomatous inflammation in various organs which subsequently progresses to fluid accumulation in the abdominal cavity and death. In contrast to more common asymptomatic or mild enteritis caused by feline enteric coronavirus, enteric biotype of FCoV, FIP is relatively uncommon in the general cat population, but it is the leading cause of death in young cats (1-3). In addition to two biotypes of feline enteric coronavirus and FIP coronavirus, FCoV are also classified into two serotypes, I and II. FCoV serotype I is more prevalent than serotype II which appears to be derived from recombination with canine coronavirus in the spike (S) protein (4-8). Both serotypes can cause enteritis or FIP in domestic and wild feline population including wildcats, cheetahs, mountain lions and leopards (9-11). Virulent, systemic (vs)-FCV is associated with systemic infection with a mortality as high as 67% (12-16). Unlike FCV associated with acute upper respiratory infection and oral ulceration, vs-FCV infection is characterized by expanded tissue tropism, causing facial and limb edema, vasculitis and multiple organ dysfunctions (12-16). Despite the importance of these virus infections in cats, no effective preventive measure is currently available [reviewed in (17)] and treatment options for FIP and vs-FCV infections are limited to supportive therapy due to the lack of specific antiviral drugs. Therefore, effective therapeutic measures such as antiviral drugs to combat these viral infections in cats are in dire need.

FCoV is an enveloped, single-stranded positive-sense RNA virus that is the member of the *Coronaviridae* family. FCV is a non-enveloped, single-stranded positive-sense RNA virus that belongs to the *Caliciviridae* family. During replication, these viruses produce one (calicivirus) or multiple (coronavirus) viral polyproteins that are cleaved into functional structural or nonstructural virus proteins by virus-encoded proteases [reviewed in (18, 19)]. Viral 3C-like protease (3CLpro) is responsible for processing of the majority of cleavage sites, thus it is essential in the replication of coronaviruses and caliciviruses. The 3CLpro encoded by those viruses shares several common characteristics, such as a typical chymotrypsin-like fold; the presence of a Cys nucleophile in the catalytic triad or dyad; and a preference for a Glu or Gln residue at the P1 position in the substrate [in the nomenclature of Schechter and Berger (20)]. Therefore, 3CLpro may serve as a potential target for the development of broad-spectrum antiviral agents for coronaviruses and caliciviruses.

We have previously synthesized peptidyl inhibitors based on the conserved key features of 3CLpro or related 3C protease (3Cpro) encoded by coronaviruses, caliciviruses or picornaviruses and reported their broad-spectrum antiviral activities against multiple viruses in the enzyme- or cell-based assay systems (21-23). However, those compounds showed minimal antiviral activity against FCV in cell culture, suggesting that further evaluation of structural-activity relationships around these peptidyl scaffolds is required for the development of broad-spectrum therapeutic agents for FCoV and FCV. In this study, we evaluated the anti-FCoV and -FCV activities of newly synthesized compounds as well as the compounds that were previously reported by us but were not tested against FCoV and FCV, and identified compounds that are effective against both FCoV and FCV in cell-based assays. The efficacies of representative dipeptidyl and tripeptidyl compounds were evaluated in mice infected with murine hepatitis virus (MHV)-A59, a hepatotrophic murine coronavirus, as a model for FIP. Our findings show that tripeptidyl compounds in general exhibit increased dual inhibitory activity against FCV and FCoV in cell culture and the dipeptidyl and tripeptidyl compounds significantly reduced viral titers and histopathological changes in the liver of mice infected with MHV compared to control group. In summary, our peptidyl compounds, especially the tripeptidyl compounds, may have the potential to be developed as antiviral therapeutics targeting both FCoV and FCV.

Materials and Methods

Compounds. To identify potential broad-spectrum inhibitors against FCoV and FCV, the 3CLpro inhibitor libraries generated by our group was evaluated. The synthesis of dipeptydyl compounds GC373, GC376, GC543, GC546, GC551, and GC554 (22, 24, 25), and tripeptidyl compounds NPI52 (compound 2), NPI59 (compound 6), NPI64 (compound 7), and NPI71 (compound 8) (23) were described previously. Compounds NPI58, NPI65 and NPI66 was synthesized by modification of the reported method (23) and were not previously reported. Compound confirmation and purity assessment was performed by NMR, mass spectrometry and HPLC in Hua's (Department of Chemistry, Kansas State University) or Groutas' Laboratories (Department of Chemistry, Wichita State University). The structures of the compounds are shown in Figure 1A and B.

Cells and viruses. Crandell-Rees Feline Kidney (CRFK) cells were maintained in Minimum Essential Medium (MEM) containing 2~5% fetal bovine serum and antibiotics of chlortetracycline (25 µg/ml), penicillin (250 U/ml), and streptomycin (250 µg/ml). FCoV WSU-79-1146, non-vs-FCV strains Urbana, 131 and F9, and vs-FCV strains 5, Ari, Deuce and Jengo were propagated in CRFK cells. CRFK cells and WSU-79-1146 were obtained from ATCC (Manassas, VA). FCV are a kind gift from Dr. J. Parker at Cornell University. WSU-79-1146 is a cell culture adapted group II FCoV which is reported to cause FIP in experimentally inoculated cats (26).

Antiviral effects of compounds in cell culture. Confluent monolayer of CRFK cells in 24-well plates were added with serial dilutions of each compound or mock and immediately inoculated with a virus at a multiplicity of infection (MOI) of 0.05 ~0.1. Cells were then further incubated at 37°C until extensive cytopathic effect was observed in the mock (untreated) well (up to 24 h). After freezing and thawing of viruses in cell culture, virus titers were determined by the 50% tissue culture infectious dose ($TCID_{50}$) method (27). Stock solutions of test compounds (10 mM) were prepared in DMSO and DMSO in cell culture did not exceed 0.5%. The 50% effective concentration (EC_{50}) values were determined by nonlinear regression analyses of dose-response curves of virus titers against log inhibitor concentrations (variable slope) using GraphPad Prism (GraphPad Software, San Diego, CA).

Nonspecific cytotoxic effect. CRFK cells in 96-well plates were incubated with each compound at various concentrations up to 150 µM for 24 h. Cell cytotoxicity was measured by a CytoTox96® nonradioactive cytotoxicity assay kit (Promega, Madison, WI) following the manufacturer's instructions. The 50% cytotoxic concentration (CC_{50}) was determined for each compound using GraphPad Prism.

Western blot analysis. CRFK cells were treated with mock or each compound and immediately infected with FCoV 1146 or FCV Urbana at an MOI of 0.5. The cells were then further incubated at 37°C for 12 h. At 12 h post infection, cells were lysed with SDS-PAGE sample buffer containing 1% β-mercaptoethanol and the proteins were resolved on 10% Novex Tris-Bis gels (Invitrogen, Carlsbad, CA) and transferred to nitrocellulose membranes. Viral proteins were probed by using a specific antibody for FCV VP1 (28) or FCoV nucleocapsid protein (Biocompare, Windham, NH) and then with peroxidase-conjugated, goat anti-mouse IgG or rabbit anti-goat IgG. β-actin was used as a loading control. Following incubation with a chemiluminescent substrate (Pierce Biotechnology, Rockford, IL), the chemiluminescent signals were detected using a Fotodyne Transilluminator/Digital Camera System (Fotodyne/FX, Hartland, WI).

Multiple sequence alignment and three dimensional structural models for 3CLpro. Multiple amino acid sequence alignment of 3CLpro from FCV Urbana (GenBank L40021.1), vs-FCV strains Jango (GenBank DQ910793.1), Ari (GenBank DQ910794.1) and Deuce (GenBank DQ91-789.1), FCoV strains 1146 (GenBank DQ010921.1), Black

(GenBank EU186072.1) and DF-2 (GenBank JQ408981.1), and MHV-A59 (GenBank NC_001846.1) was performed using the ClustalW multiple sequence alignment program. FCoV 1146, Black and DF-2 strains are the FIP-causing FCoV. The three dimensional structure of FCoV 3CLpro was built by EasyModeller 4.0 (29) using 3CLpro structure of transmissible gastroenteritis virus (TGEV), a porcine coronavirus, (Protein Data Bank code 2AMP) as a template. FCV 3CLpro three-dimensional structure was built by EasyModeller using rhinovirus 3Cpro, poliovirus 3Cpro, human norovirus 3CLpro, and hepatitis A virus 3Cpro (Protein Data Bank code 1CQQ, 1L1N, 2LNC, and 1QA7, respectively)(30) as templates. The quality of the models were assessed using Verify 3D (31).

Animal experiments. The animal study was performed in accordance with a protocol approved by the Institutional Animal Care and Use Committee (IACUC) at Kansas State University. BALB/c mice were purchased from Charles River Lab (Wilmington, MA). Prior to animal experiments, the In EC_{50} values of GC376 and NPI52 against MHV-A59 were determined to be 0.2~1 μM in CCL9.1 mouse liver cells. To confirm MHV-A59 infection induces consistent and high virus replication in the liver of the infected mice, we inoculated 4-5 week-old female BALB/c mice intraperitoneally with MHV-A59 at $7.2x10^4$ or $5.2x10^5$ $TCID_{50}$/mouse. At 2 and 4 days post-infection (dpi), mice were sacrificed (4-6 mice/group), and the livers were collected and processed for virus titration by the $TCID_{50}$ method. For *in vivo* efficacy study, 4-5 week-old female BALB/c mice were inoculated intraperitoneally with MHV-A59 at $7.2x10^4$ or $5.2x10^5$ $TCID_{50}$/mouse. Mice were intraperitoneally given 50 μl of drug vehicle (10% EtOH, 70%

PEG400 and 20% PBS), GC376 (10, 50 or 100 mg/kg/day) or NPI52 (10 or 100 mg/kg/day) divided into two doses per day. Compound administration started 4 h prior to virus infection and continued daily until mice were euthanized. At 2 and 4 dpi, mice were sacrificed and the livers were collected and processed for virus titration. Virus titers were determined by the $TCID_{50}$ method and the liver virus titers were compared by two-tailed student's t-test. Fold changes in the geometric mean liver virus titers in each group were calculated by dividing virus titers in control group by those of treated group.

Liver histopathology. The left lateral lobes were collected at 4 dpi from NPI52-treated mice (10 and 100 mg/kg/day), formalin-fixed, embedded in paraffin, sectioned and stained with hematoxylin and eosin for histopathological examination by a board-certified pathologist. Five views were examined per mouse liver and a score from 0 to 5 was assigned to each lesion contained in the view based on the severity of histopathological changes. Each score in each sample was added to give a final total score and then the mean of total scores per sample was calculated for each group. The mean number of lesions per sample was also calculated for each group. The mean total score per sample and the mean number of lesions per sample were compared among different experimental groups using two-tailed student's t-test.

Results

Antiviral effects of dipeptidyl and tripeptidyl compounds on the replication of FCoV and FCV. We evaluated dipeptidyl and tripeptidyl compounds with varying R^1

and R^2 side chains against FCoV 1146 and FCV Urbana in cell culture (Figure 1A and B). For dipeptidyl compounds, replacing R^2 isobutyl (Leu side chain) with benzyl (Phe side chain) or cyclohexylmethyl (Cha side chain) on a representative dipeptidyl compound, GC373, increased anti-FCV activity while decreasing its potency toward FCoV. GC373 was previously shown to have potent anti-FCoV activity with minimal activity against FCV in cell culture (22). The tripeptidyl compound NPI52 has an additional residue of 1-naththylalanine compared to GC373 at the P3 position and its activity against FCoV or FCV has not been previously tested (23). In this study, we found that NPI52 exhibited potent anti-FCoV and anti-FCV activity with EC_{50} values in the nanomolar range (Figure 1A), which indicates that the presence of the additional residue at the P3 subsite dramatically increased its activity against FCV. When R^2 isobutyl was replaced with benzyl or cyclohexylmethyl in NPI52, benzyl substitution decreased anti-FCoV activity more than cyclohexylmethyl, but similar reduction in anti-FCV activity was observed compared to GC373. Replacement of the aldehyde warhead in NPI52 with ketoamides [(C=O)(C=O)NHCH$(CH_3)_2$ or (C=O)(C=O)NHC$(CH_3)_3$] greatly decreased anti-FCV activity but their activity against FCoV was only moderately decreased. Similarly, replacement of aldehyde with α-hydroxy phosphonate [CH(OH)P(O)$(OCH_2CH_3)_2$] greatly decreased anti-FCV activity with only a minor effect on anti-FCoV activity. NPI64, GC376, GC551 and GC554 are bisulfite adducts of NPI52, GC373, GC543 and GC546, respectively, and they showed comparable antiviral activities against FCoV and FCV to their aldehyde counterparts in cell culture. The CC_{50} values of all compounds ranged from 21.96 to higher than 150 μM in CRFK cells (Figure

1A and B). Western blot analysis confirmed the effects of our compounds on the expression of FCoV nucleocapsid protein or FCV VP1 (Figure 2).

Compound NPI52 that possesses potent antiviral effects against both FCoV 1146 and FCV Urbana was also tested against other non-vs-FCV and vs-FCV in cell culture to determine whether this compound is effective against various FCV strains. The EC_{50} values in Table 1 show that NPI52 potently inhibits the replication of various non-vs-FCV and vs-FCV in cell culture.

Multiple sequence alignment and three dimensional structural models for 3CLpro. The amino acid sequences of 3CLpro have the high sequence homology of >95% within FCV or FCoV (Figure 3A and C). However, there are substantial differences in their sequences (19.72% homology) between FCV and FCoV 3CLpro. Although the sequence homology between FCV and FCoV 3CLpro is low, the catalytic residues are well-conserved (Figure 3A-D). MHV-A59 3CLpro shares the amino acid homology of 47.35% with FCoV 3CLpro and the locations of catalytic residues (red arrow heads) well correspond to those of FCoV strains (Figure 3C). The residues in the catalytic dyad or triad are shown in the blue box (Figure 3B and D).

***In vivo* efficacy of compounds in coronavirus-infected mice.** Intraperitoneal inoculation of MHV-A59 at 7.2×10^4 or 5.2×10^5 $TCID_{50}$/mouse led to high virus replication in the liver and the levels of virus replication were not significantly different between two virus inoculums determined by two-tailed student t-test ($p < 0.05$) (data not shown). In the *in vivo* efficacy study, NPI52 and GC376 were tested in mice infected with MHV-A59.

In two separate experiments where mice were treated with GC376 or mock, the liver virus titers in mice treated with GC376 at 50 or 100 mg/kg were significantly lower than no-treatment control at 4 dpi, but not at 2 dpi ($p < 0.05$) (Figure 4A and B). The fold-reductions of geometric mean virus titers in mice received GC376 at 50 or 100 mg/kg at 4 dpi were 9.86 and 21.99, respectively, compared to the control (Figure 4A and B, bar graphs). In contrast, GC376 at 10 mg/kg did not consistently lead to a significant reduction in virus titers at both time points.

In two independent NPI52-treatment experiments, NPI52 100 mg/kg resulted in significant reduction of liver virus titers at 4 dpi with fold-reductions of 19.63-40.27 and at 2 dpi with fold-reductions of 3.46-12.3 compared to the control (Figure 4C and D). However, NPI52 10 mg/kg failed to significantly reduce virus titers compared to the control at 2 dpi or 4 dpi (Figure 4C and D), although significant viral reduction was observed at 4 dpi in one of the experiment (Figure 4C and D). The mock-infected mice did not show any sign of illness during the duration of the experiments and no gross pathological lesion was observed on necropsy.

Histopathology of liver. Figure 5A panels represent scores 0 through 5 with increasing histopathology severity. Based on the lesion scoring, NPI52 100 mg/kg-treated group had significantly lower mean number of lesions and mean total histopathology scores per mouse liver compared to the control (Figure 5B and D). There was no statistical difference for the mean total histopathology scores and the mean number of lesions between the control and NPI52 10 mg/kg-treated group. However, the lesions in all drug-treated groups were scored 3 or lower, which is in contrast to the presence of lesions scored 4 or 5 in no-treatment control group (Figure 5C). Of note, the liver section from a mouse in NPI52 10 mg/kg group did not contain any histopathology lesion and was excluded from statistical analysis in Figure 5B-D. Examination of the liver samples from mock-infected mice revealed no significant microscopic lesions associated with compound toxicity.

Discussion

Although infections with FCoV or FCV generally are asymptomatic or cause mild localized symptoms in cats, they can also cause systemic diseases with high fatality, which are increasingly important causes of death among cats. These viruses are distinct in their genome organization, virus properties and pathogenesis, but they share the dependency on viral proteases during replication for production of functional structural or non-structural virus proteins from viral polyprotein(s). The amino acid sequence homology between FCV and FCoV 3CLpro is less than 20%, however, they have similar active site configuration (Figure 3A-D) (22, 30, 32). Based on the highly conserved key site of 3CLpro expressed by coronaviruses and caliciviruses, we have previously synthesized peptidyl compounds and identified compounds that exhibit broad-spectrum antiviral efficacy against viruses in the *Coronaviridae* and *Caliciviridae* families and also against viruses in the *Picornaviridae* family that encode closely related 3Cpro (22). The dipeptidyl compounds that were previously evaluated for broad-spectrum antiviral effects consist of a warhead, a Gln surrogate structure in a position that corresponds to the P1 position, Leu in the P2 position and a cap structure. These compounds have

EC_{50} values in the nanomolar or low micromolar range against many members of caliciviruses, picornaviruses and coronaviruses, including FCoV (22). These findings demonstrated that 3CLpro could serve as a target for the development of broad-spectrum antiviral agents for viruses encoding 3CLpro or 3Cpro. However, these compounds were only minimally effective against FCV in cell culture (with EC_{50} >30 µM) (22) and their low activity was speculated to be due to space constraints in the S2 pocket in the 3CLpro of FCV.

In the present study, we evaluated newly synthesized and previously reported dipeptidyl and tripeptidyl compounds that were not previously tested against FCoV and FCV in cell culture. Our findings showed that the presence of an additional residue in NPI52 remarkably enhances the anti-FCV activity while maintaining potency against FCoV compared to dipeptidyl compounds (including GC373), suggesting that tripeptidyl compounds may provide a more suitable platform for dual-spectrum antiviral drug design for FCoV and FCV. Our limited structure-activity relationship study revealed that replacing Leu side chain at the P2 site or warhead on dipeptidyl or tripeptidyl compounds changed the antiviral activity against FCoV and FCV at varying degrees. The effects of different warheads on the tripeptidyl compound were more profound on the antiviral activity against FCV than FCoV, which may suggest that the interaction of warhead and the nucleophile Cys in the active site of FCV 3CLpro may require more stringent fit at the active site than FCoV. Further investigation, such as crystallographic studies with inhibitor-3CLpro complexes of FCoV or FCV may illuminate the structural basis of our findings. Among our tested compounds, NPI64, GC376, GC551 and GC554 are bisulfite adducts of NPI52, GC373, GC543 and GC546, respectively, and they showed comparable antiviral activities against FCoV and FCV to their aldehyde counterparts in cell culture. Bisulfite adduct compound GC376 was previously reported to be dissociated into the corresponding aldehyde (GC373) and bisulfite ion when incubated with 3CLpro, with the resulting aldehyde subsequently forming a covalent adduct with the active site Cys of 3CLpro in X-ray crystallographic studies (22). We also observed facile transformation of GC376 and NPI64 to their respective aldehyde forms in the blood of rats and cats in our preliminary animal studies (data not shown). These observations suggest that the bisulfite adduct compounds may act as prodrugs with the active aldehyde metabolites in cell culture and animals.

We also determined the antiviral effects of NPI52 on the replication of various vs-FCV as well as non-vs-FCV strains in cell culture to determine the sensitivity of various strains of FCV to the compound. The results showed that the potency of NPI52 against four vs-FCV strains are generally lower than against non-vs-FCV strains, but it still remained high with EC_{50} values in the nanomolar range. The higher EC_{50} values of NPI52 against vs-FCV may be attributed to faster multi-cycle growth kinetics of vs-FCV strains leading to higher yields of virus progeny than non-vs-FCV strains (33). These results indicate that our compounds may be of potential therapeutic value for the treatment of highly fatal vs-FCV infection as well as non-vs-FCV infection that is an important cause of respiratory diseases and oral ulceration in cats. The compounds have minimal or low cytotoxicity in CRFK cells; the CC_{50} values of dipeptidyl compounds are greater than 150 µM with the *in vitro* therapeutic indexes (TIs) of higher than 349 to 7,500. Tripeptidyl compounds also have good TIs, but they are lower than dipeptidyl compound: the compounds with $EC_{50} < 1$ µM against FCoV or FCV have TIs ranged from 31.8 to 3,514 (Figure 1A). The *in vitro* TIs are expressed as a ratio of CC_{50} to EC_{50}, and these results indicate that our compounds have relatively high *in vitro* safety margins and can be suitable candidates for *in vivo* studies.

A number of classes of inhibitors of coronavirus 3CLpro have been identified in a cell culture system or in an enzyme assay since the systemic acute respiratory syndrome (SARS)-coronavirus outbreaks in 2003 (34-41). However, few studies have reported the efficacy of coronavirus 3CLpro inhibitors in experimental animals. Therefore, we evaluated a dipeptidyl (GC376) and a tripeptidyl (NPI52) compounds in mice infected with a murine coronavirus, MHV. MHV causes systemic diseases including hepatitis and a variety of immunological dysfunctions in mice. Specifically, MHV-A59 inoculation of mice by a peritoneal route causes severe liver disease and multi-organ infections (42, 43). This animal model was used as surrogate model for FIP since feline coronavirus naturally infects only members of the family *Felidae*. In our study, the antiviral effects of GC376 and NPI52 were dose-dependent in reducing liver viral titers compared to no-treatment control group and statistically significant reduction in viral load in the liver was consistently observed at 4 dpi with higher doses of GC376 or NPI52 (Figure 4A-D). It is also important to note that GC376 and NPI52 have much weaker activity against MHV-A59 compared to FCoV in cell culture (at least 10 fold-higher EC_{50} values). Nonetheless, the compounds showed marked antiviral activity against MHV (up to 40-fold reduction in virus load) without causing toxicity in mice.

Histopathology examination of the liver samples of mice treated with NPI52 or mock demonstrated that NPI52 100 mg/kg significantly reduced the mean total scores and the mean number of lesions in the livers of mice treated with NPI52, compared to no-treatment control group. There was no statistical difference for the mean total histopathology scores and the mean number of lesions between the no-treatment control and 10 mg/kg-treated group. However, all groups treated with NPI52 had no lesion scored 4 and above, indicating that NPI52 treatment at both doses inhibited the expansion of the lesions in the liver, since lesions develop as small foci and adjacent foci coalesce to form larger lesions. These *in vivo* results demonstrated that inhibition of coronavirus 3CLpro is a valid therapeutic approach to suppress coronavirus replication and virus-induced pathology.

In summary, we synthesized and tested derivatives of peptidyl compounds that target 3CLpro and identified compounds with dual antiviral activity against FCoV and FCV in cell culture. Their efficacy in a mouse model for coronavirus infection and a wide safety margin in cell culture suggest that these compounds may be suitable for further investigation as a broad-spectrum antiviral drug targeting 3CLpro for FCoV and FCV.

Acknowledgements

This work was supported by Winn Feline Foundation grant W13-020, Morris Animal Foundation grant D14FE-012, and NIH grants U01AI081891 and R01AI109039.

We thank David George and Takashi Taguchi for technical assistance. We also thank Dr. Tracy Miesner and Comparative Medicine Group for their support for animal research.

References

1. **Rohrbach BW, Legendre AM, Baldwin CA, Lein DH, Reed WM, Wilson RB.** 2001. Epidemiology of feline infectious peritonitis among cats examined at veterinary medical teaching hospitals. J Am Vet Med Assoc **218:**1111-1115.
2. **Foley JE, Poland A, Carlson J, Pedersen NC.** 1997. Risk factors for feline infectious peritonitis among cats in multiple-cat environments with endemic feline enteric coronavirus. J Am Vet Med Assoc **210:**1313-1318.
3. **Pedersen NC.** 2009. A review of feline infectious peritonitis virus infection: 1963-2008. J Feline Med Surg **11:**225-258.
4. **Benetka V, Kubber-Heiss A, Kolodziejek J, Nowotny N, Hofmann-Parisot M, Mostl K.** 2004. Prevalence of feline coronavirus types I and II in cats with histopathologically verified feline infectious peritonitis. Vet Microbiol **99:**31-42.
5. **Pedersen NC, Black JW, Boyle JF, Evermann JF, McKeirnan AJ, Ott RL.** 1984. Pathogenic differences between various feline coronavirus isolates. Adv Exp Med Biol **173:**365-380.
6. **Kummrow M, Meli ML, Haessig M, Goenczi E, Poland A, Pedersen NC, Hofmann-Lehmann R, Lutz H.** 2005. Feline coronavirus serotypes 1 and 2: seroprevalence and association with disease in Switzerland. Clin Diagn Lab Immunol **12:**1209-1215.
7. **Motokawa K, Hohdatsu T, Hashimoto H, Koyama H.** 1996. Comparison of the amino acid sequence and phylogenetic analysis of the peplomer, integral membrane and nucleocapsid proteins of feline, canine and porcine coronaviruses. Microbiol Immunol **40:**425-433.
8. **Herrewegh AA, Smeenk I, Horzinek MC, Rottier PJ, de Groot RJ.** 1998. Feline coronavirus type II strains 79-1683 and 79-1146 originate from a double recombination between feline coronavirus type I and canine coronavirus. J Virol **72:**4508-4514.
9. **Stephenson N, Swift P, Moeller RB, Worth SJ, Foley J.** 2013. Feline infectious peritonitis in a mountain lion (Puma concolor), California, USA. J Wildl Dis **49:**408-412.
10. **Heeney JL, Evermann JF, McKeirnan AJ, Marker-Kraus L, Roelke ME, Bush M, Wildt DE, Meltzer DG, Colly L, Lukas J, et al.** 1990. Prevalence and implications of feline coronavirus infections of captive and free-ranging cheetahs (Acinonyx jubatus). J Virol **64:**1964-1972.
11. **Kennedy M, Citino S, McNabb AH, Moffatt AS, Gertz K, Kania S.** 2002. Detection of feline coronavirus in captive Felidae in the USA. J Vet Diagn Invest **14:**520-522.
12. **Hurley KE, Pesavento PA, Pedersen NC, Poland AM, Wilson E, Foley JE.** 2004. An outbreak of virulent systemic feline calicivirus disease. J Am Vet Med Assoc **224:**241-249.
13. **Pedersen NC, Elliott JB, Glasgow A, Poland A, Keel K.** 2000. An isolated epizootic of hemorrhagic-like fever in cats caused by a novel and highly virulent strain of feline calicivirus. Vet Microbiol **73:**281-300.
14. **Foley J, Hurley K, Pesavento PA, Poland A, Pedersen NC.** 2006. Virulent systemic feline calicivirus infection: local cytokine modulation and contribution of viral mutants. J Feline Med Surg **8:**55-61.
15. **Schulz BS, Hartmann K, Unterer S, Eichhorn W, Majzoub M, Homeier-Bachmann T, Truyen U, Ellenberger C, Huebner J.** 2011. Two outbreaks of virulent systemic feline calicivirus infection in cats in Germany. Berl Munch Tierarztl Wochenschr **124:**186-193.
16. **Reynolds BS, Poulet H, Pingret JL, Jas D, Brunet S, Lemeter C, Etievant M, Boucraut-Baralon C.** 2009. A nosocomial outbreak of feline calicivirus associated virulent systemic disease in France. J Feline Med Surg **11:**633-644.

17. **Pedersen NC.** 2014. An update on feline infectious peritonitis: Diagnostics and therapeutics. Vet J **201:**133-141.

18. **Ziebuhr J, Snijder EJ, Gorbalenya AE.** 2000. Virus-encoded proteinases and proteolytic processing in the Nidovirales. J Gen Virol **81:**853-879.

19. **Green KY.** 2007. Caliciviruses: the Noroviruses, 5th ed, vol. 1. Lippincott Williams & Wilkins, Philadelphia.

20. **Schechter I, Berger A.** 1967. On the size of the active site in proteases. I. Papain. Biochem Biophys Res Commun **27:**157-162.

21. **Kim Y, Mandadapu SR, Groutas WC, Chang K-O.** 2013. Potent Inhibition of Feline Coronaviruses with Peptidyl Compounds Targeting Coronavirus 3C-like Protease. Antiviral Research **97:**161.

22. **Kim Y, Lovell S, Tiew KC, Mandadapu SR, Alliston KR, Battaile KP, Groutas WC, Chang KO.** 2012. Broad-spectrum antivirals against 3C or 3C-like proteases of picornaviruses, noroviruses, and coronaviruses. J Virol **86:**11754-11762.

23. **Prior AM, Kim Y, Weerasekara S, Moroze M, Alliston KR, Uy RA, Groutas WC, Chang KO, Hua DH.** 2013. Design, synthesis, and bioevaluation of viral 3C and 3C-like protease inhibitors. Bioorg Med Chem Lett **23:**6317-6320.

24. **Tiew KC, He G, Aravapalli S, Mandadapu SR, Gunnam MR, Alliston KR, Lushington GH, Kim Y, Chang KO, Groutas WC.** 2011. Design, synthesis, and evaluation of inhibitors of Norwalk virus 3C protease. Bioorg Med Chem Lett **21:**5315-5319.

25. **Mandadapu SR, Gunnam MR, Tiew KC, Uy RA, Prior AM, Alliston KR, Hua DH, Kim Y, Chang KO, Groutas WC.** 2013. Inhibition of norovirus 3CL protease by bisulfite adducts of transition state inhibitors. Bioorg Med Chem Lett **23:**62-65.

26. **Pedersen NC, Evermann JF, McKeirnan AJ, Ott RL.** 1984. Pathogenicity studies of feline coronavirus isolates 79-1146 and 79-1683. Am J Vet Res **45:**2580-2585.

27. **Reed LJ, Muench H.** 1938. A simple method of estimating fifty percent endpoints. The American Journal of Hygiene **27:**493-497.

28. **Sosnovtsev S, Green KY.** 1995. RNA transcripts derived from a cloned full-length copy of the feline calicivirus genome do not require VpG for infectivity. Virology **210:**383-390.

29. **Kuntal BK, Aparoy P, Reddanna P.** 2010. EasyModeller: A graphical interface to MODELLER. BMC Res Notes **3:**226.

30. **Oka T, Yamamoto M, Yokoyama M, Ogawa S, Hansman GS, Katayama K, Miyashita K, Takagi H, Tohya Y, Sato H, Takeda N.** 2007. Highly conserved configuration of catalytic amino acid residues among calicivirus-encoded proteases. J Virol **81:**6798-6806.

31. **Bowie JU, Luthy R, Eisenberg D.** 1991. A method to identify protein sequences that fold into a known three-dimensional structure. Science **253:**164-170.

32. **Anand K, Ziebuhr J, Wadhwani P, Mesters JR, Hilgenfeld R.** 2003. Coronavirus main proteinase (3CLpro) structure: basis for design of anti-SARS drugs. Science **300:**1763-1767.

33. **Ossiboff RJ, Sheh A, Shotton J, Pesavento PA, Parker JS.** 2007. Feline caliciviruses (FCVs) isolated from cats with virulent systemic disease possess in vitro phenotypes distinct from those of other FCV isolates. J Gen Virol **88:**506-517.

34. **Ramajayam R, Tan KP, Liu HG, Liang PH.** 2010. Synthesis and evaluation of pyrazolone compounds as SARS-coronavirus 3C-like protease inhibitors. Bioorg Med Chem **18:**7849-7854.

35. **Bacha U, Barrila J, Gabelli SB, Kiso Y, Mario Amzel L, Freire E.** 2008. Development of broad-spectrum halomethyl ketone inhibitors against coronavirus main protease 3CL(pro). Chem Biol Drug Des **72:**34-49.

36. **Liang PH.** 2006. Characterization and inhibition of SARS-coronavirus main protease. Curr Top Med Chem **6:**361-376.

37. **Kuo CJ, Liu HG, Lo YK, Seong CM, Lee KI, Jung YS, Liang PH.** 2009. Individual and common inhibitors of coronavirus and picornavirus main proteases. FEBS Lett **583:**549-555.

38. **Yang H, Xie W, Xue X, Yang K, Ma J, Liang W, Zhao Q, Zhou Z, Pei D, Ziebuhr J, Hilgenfeld R, Yuen KY, Wong L, Gao G, Chen S, Chen Z, Ma D, Bartlam M, Rao Z.** 2005. Design of wide-spectrum inhibitors targeting coronavirus main proteases. PLoS Biol **3:**e324.

39. **Yamamoto N, Yang R, Yoshinaka Y, Amari S, Nakano T, Cinatl J, Rabenau H, Doerr HW, Hunsmann G, Otaka A, Tamamura H, Fujii N, Yamamoto N.** 2004. HIV protease inhibitor nelfinavir inhibits replication of SARS-associated coronavirus. Biochem Biophys Res Commun **318:**719-725.

40. **Ghosh AK, Gong G, Grum-Tokars V, Mulhearn DC, Baker SC, Coughlin M, Prabhakar BS, Sleeman K, Johnson ME, Mesecar AD.** 2008. Design, synthesis and antiviral efficacy of a series of potent chloropyridyl ester-derived SARS-CoV 3CLpro inhibitors. Bioorg Med Chem Lett **18:**5684-5688.

41. **Agnihothram S, Yount BL, Jr., Donaldson EF, Huynh J, Menachery VD, Gralinski LE, Graham RL, Becker MM, Tomar S, Scobey TD, Osswald HL, Whitmore A, Gopal R, Ghosh AK, Mesecar A, Zambon M, Heise M, Denison MR, Baric RS.** 2014. A mouse model for Betacoronavirus subgroup 2c using a bat coronavirus strain HKU5 variant. MBio **5:**e00047-00014.

42. **Hingley ST, Leparc-Goffart I, Weiss SR.** 1998. The mouse hepatitis virus A59 spike protein is not cleaved in primary hepatocyte and glial cell cultures. Adv Exp Med Biol **440:**529-535.

43. **Kim KD, Zhao J, Auh S, Yang X, Du P, Tang H, Fu YX.** 2007. Adaptive immune cells temper initial innate responses. Nat Med **13:**1248-1252.

Figure legends

Figure 1. Chemical structures of tripeptidyl (A) and dipeptidyl compounds (B) and the mean and the standard error of the means (SEM) of the EC_{50} values of compounds against FCoV or FCV. Each compound was added to CRFK cells and the cells were immediately infected with FCoV 1146 or FCV Urbana. Cells were further incubated in the presence of each compound for up to 24 h. Virus titers were determined using the $TCID_{50}$ method and the EC_{50} values were calculated. Compound cytotoxicity (CC_{50}) was measured after incubating cells with each compound for 24 h.

Figure 2. Western blot analysis of the effects of the compounds on the expression of FCoV nucleocapsid protein or FCV VP1 in CRFK cells. Cells were treated with mock or each compound and immediately infected with FCoV 1146 or FCV Urbana. The cells were then further incubated for 12 h. Cell lysates were prepared and analyzed for expression of viral proteins on Western blot. β-actin was used as a loading control.

Figure 3. Multiple sequence alignments for 3CLpro from FCV (A) and FCoV and MHV-A59 (C) and ribbon presentations of three dimensional structural models for FCV (B) and FCoV 3CLpro (D). (A and C) The catalytic residues E60, C122, and H39 of FCV 3CLpro (A) and H41 and C144 of FCoV and MHV-A59 3CLpro are indicated by red arrow heads (C). (B and D) The structure model of FCoV 3CLpro was built by EasyModeller 4.0 (29) using 3CLpro structure of TGEV (Protein Data Bank code 2AMP) as a template. The structure model of FCV 3CLpro was built by EasyModeller using

3Cpro of rhinovirus, poliovirus, human norovirus, and hepatitis A virus (Protein Data Bank code 1CQQ, 1L1N, 2LNC, and 1QA7, respectively)(30) as templates. The amino acids in the catalytic triad (E60, C122, and H39 for FCV 3CLpro) (B) and dyad (H41 and C144 for FCoV 3CLpro) (C) are shown in the blue box.

Figure 4. Effects of 3CLpro inhibitor treatment on MHV-A59 titers. Four to five week-old BALB/c mice were intraperitoneally inoculated with MHV-A59 at 5.2×10^5 (A) or 7.2×10^4 (B-D) $TCID_{50}$/mouse and treated with drug vehicle, GC376 (10, 50 or 100 mg/kg/day) or NPI52 (10 or 100 mg/kg/day) divided into two doses per day starting at 4 h prior to virus infection. Scatter plots show mean and the standard error of the means of virus titers in the liver of mice received mock (drug vehicle), GC376 (A and B) or NPI52 (C and D) at 2 or 4 days post virus infection. Virus titers are expressed as $\log_{10}$ $TCID_{50}$ per gram of liver tissue. Bar graphs show the fold reduction of geometric mean of virus titers in treatment groups compared to the control. Asterisks indicate significant differences between the control and the treated group (* $p < 0.05$, ** $p < 0.01$).

Figure 5. Histopathology changes in the liver of mice treated with NPI52. (A) Panels representing scores 0 through 5 with increasing severity of microscopic lesions. Score 0, minimal change; scores 1-2, multifocal areas of necrosis; and scores 3-5, coalescing areas of necrosis. (B) A box and whisker plot showing the mean total liver histopathology score for each group. (C) A table showing the frequency of histopathology scores in four (NPI52 10mg/kg) or five (control and NPI52 100mg/kg)

liver samples per group. (D) A box and whisker plots showing the mean number of lesions per mouse liver for each group. Asterisks indicate statistically significant differences between control and NPI52 100 mg/kg-treated mice ($p < 0.05$). The whiskers represent 5% and 95% confidence intervals and the boxes represent 25% and 75% confidence intervals. The middle lines represent the median of the data.

Table 1. The mean and the standard error of the mean (SEM) of the EC_{50} values of NPI52 against FCV or vs-FCV strains.

	vs-FCV				FCV		
	Jengo	**5**	**Ari**	**Deuce**	**131**	**F9**	**Urbana**
EC_{50} (µM)	0.03±0.01	0.35±0.27	0.10±0.09	0.22±0.002	0.05±0.03	0.05±0.05	0.02±0.01

A

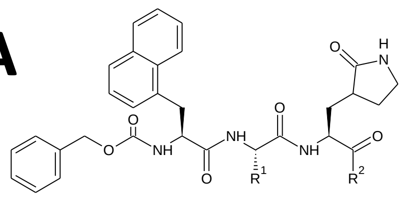

Compounds	R^1	R^2	FCoV ($EC_{50,}$ µM)	FCV ($EC_{50,}$ µM)	CC_{50} (µM)
NPI52	CHO	Isobutyl (Leu)	0.02±0.01	0.02±0.01	70.29±5.6
NPI58	CHO	Benzyl (Phe)	0.86±0.72	0.69±0.03	40.57±10
NPI59	$(C{=}O)(C{=}O)NHCH(CH_3)_2$	Isobutyl (Leu)	0.54±0.28	>5	32.34±1.9
NPI64	$CH(OH)\ SO_3Na$	Isobutyl (Leu)	0.04±0.03	0.08±0.01	61.91±0.2
NPI65	$(C{=}O)(C{=}O)NHC(CH_3)_3$	Isobutyl (Leu)	0.18±0.12	3.3±5.0	32.01±1.3
NPI66	CHO	Cyclohexylmet hyl (Cha)	0.06±0.06	0.58±0.19	21.96±5.1
NPI71	$CH(OH)P(O)(OCH_2CH_3)_2$	Isobutyl (Leu)	0.06±0.001	4.10±1.15	>150

Figure 1. Chemical structures of tripeptidyl (A) and dipeptidyl compounds (B) and the mean and the standard error of the means (SEM) of the EC_{50} values of compounds against FCoV or FCV. Each compound was added to CRFK cells and the cells were immediately infected with FCoV 1146 or FCV Urbana. Cells were further incubated in the presence of each compound for up to 24 h. Virus titers were determined using the $TCID_{50}$ method and the EC_{50} values were calculated. Compound cytotoxicity (CC_{50}) was measured after incubating cells with each compound for 24 h.

B

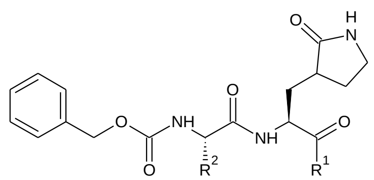

Compounds	R^1	R^2	FCoV ($EC_{50,}$ μM)	FCV ($EC_{50,}$ μM)	CC_{50} (μM)
GC373	CHO	Isobutyl (Leu)	0.02±0.01	>5	>150
GC376	CH(OH) SO_3Na	Isobutyl (Leu)	0.04±0.04	>5	>150
GC543	CHO	Cyclohexylmethyl (Cha)	0.10±0.03	5.35±3.91	>150
GC546	CHO	Benzyl (Phe)	0.43±0.31	2.09±1.59	>150
GC551	CH(OH) SO_3Na	Cyclohexylmethyl (Cha)	0.06±0.05	3.77±0.58	>150
GC554	CH(OH) SO_3Na	Benzyl (Phe)	0.12±0.05	6.0±2.082	>150

Figure 1. Chemical structures of tripeptidyl (A) and dipeptidyl compounds (B) and the mean and the standard error of the means (SEM) of the EC_{50} values of compounds against FCoV or FCV. Each compound was added to CRFK cells and the cells were immediately infected with FCoV 1146 or FCV Urbana. Cells were further incubated in the presence of each compound for up to 24 h. Virus titers were determined using the $TCID_{50}$ method and the EC_{50} values were calculated. Compound cytotoxicity (CC_{50}) was measured after incubating cells with each compound for 24 h.

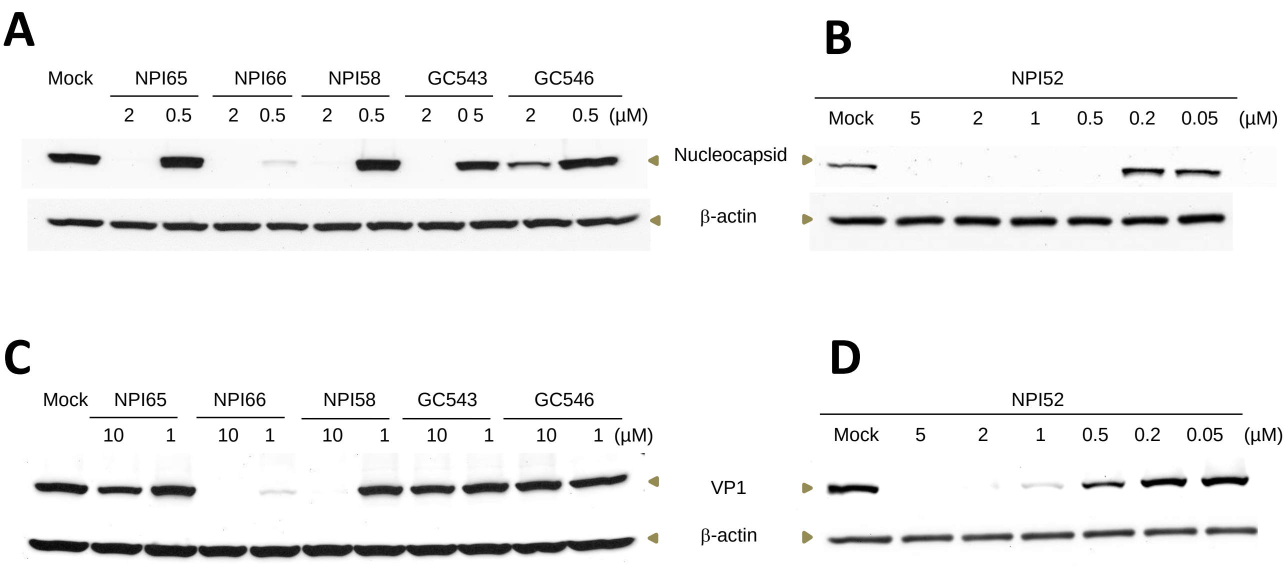

Figure 2. Western blot analysis of the effects of the compounds on the expression of FCoV nucleocapsid protein or FCV VP1 in CRFK cells. Cells were treated with mock or each compound and immediately infected with FCoV 1146 or FCV Urbana. The cells were then further incubated for 12 h. Cell lysates were prepared and analyzed for expression of viral proteins on Western blot. β-actin was used as a loading control.

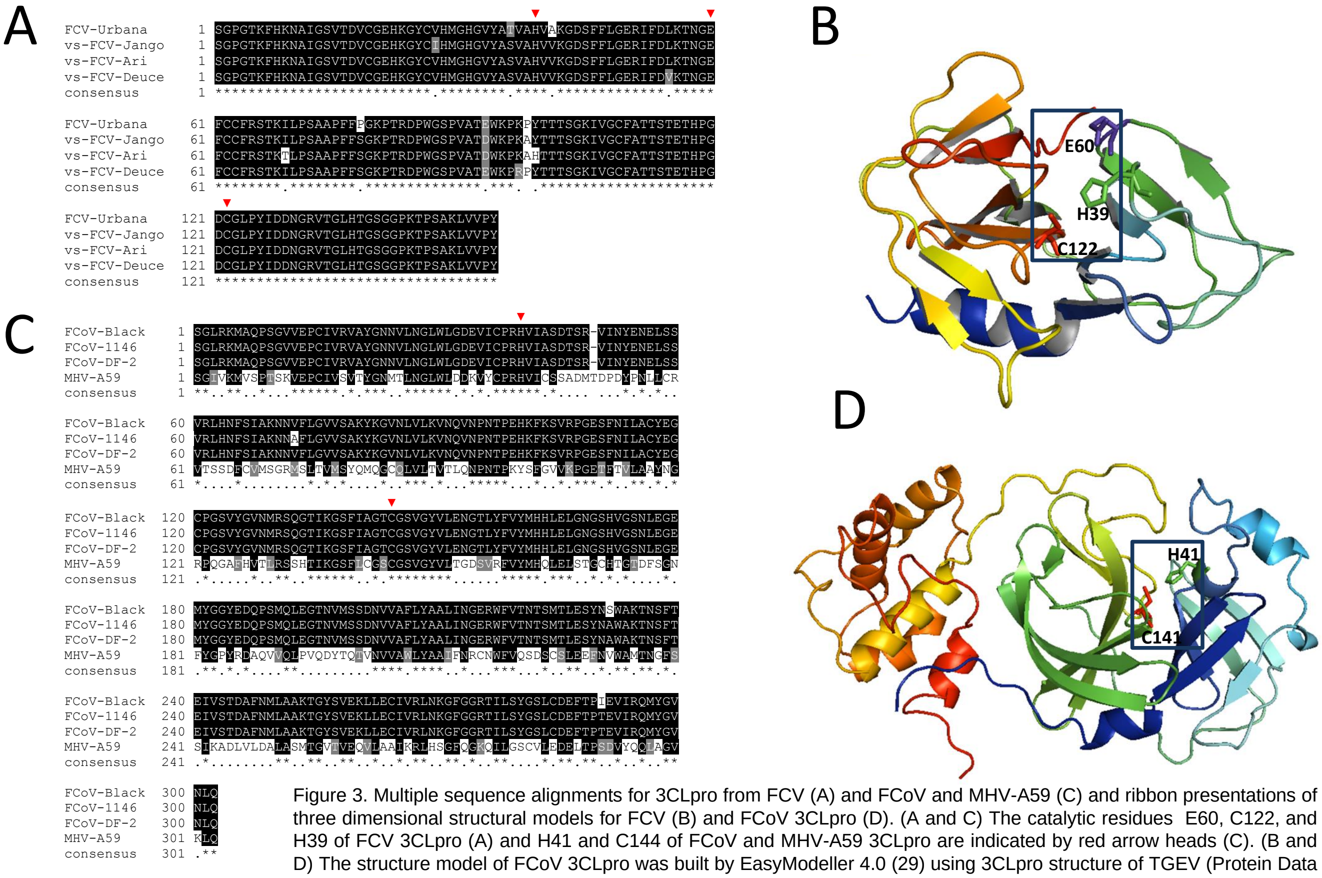

Figure 3. Multiple sequence alignments for 3CLpro from FCV (A) and FCoV and MHV-A59 (C) and ribbon presentations of three dimensional structural models for FCV (B) and FCoV 3CLpro (D). (A and C) The catalytic residues E60, C122, and H39 of FCV 3CLpro (A) and H41 and C144 of FCoV and MHV-A59 3CLpro are indicated by red arrow heads (C). (B and D) The structure model of FCoV 3CLpro was built by EasyModeller 4.0 (29) using 3CLpro structure of TGEV (Protein Data Bank code 2AMP) as a template. The structure model of FCV 3CLpro was built by EasyModeller using 3Cpro of rhinovirus, poliovirus, human norovirus, and hepatitis A virus (Protein Data Bank code 1CQQ, 1L1N, 2LNC, and 1QA7, respectively)(30) as templates. The amino acids in the catalytic triad (E60, C122, and H39 for FCV 3CLpro) (B) and dyad (H41 and C144 for FCoV 3CLpro) (D) are shown in the blue box.

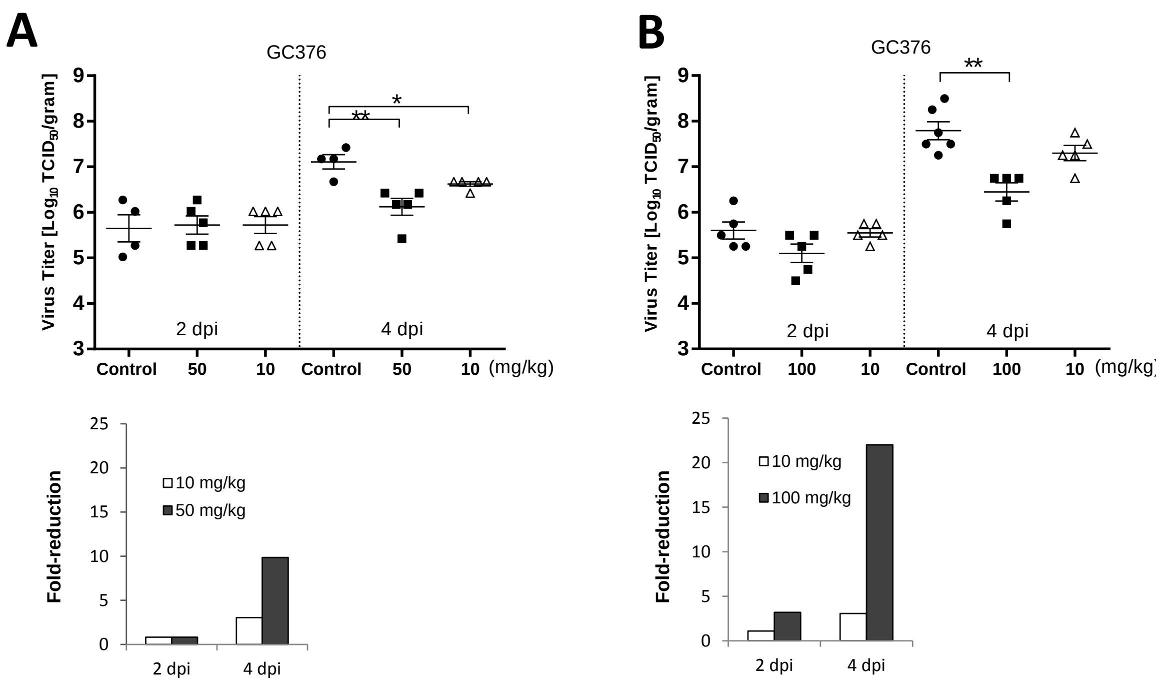

Figure 4. Effects of 3CLpro inhibitor treatment on MHV-A59 titers. Four to five week-old BALB/c mice were intraperitoneally inoculated with MHV-A59 at 5.2×10^5 (A) or 7.2×10^4 (B-D) $TCID_{50}$/mouse and treated with drug vehicle, GC376 (10, 50 or 100 mg/kg/day) or NPI52 (10 or 100 mg/kg/day) divided into two doses per day starting at 4 h prior to virus infection. Scatter plots show mean and the standard error of the means of virus titers in the liver of mice received mock (drug vehicle), GC376 (A and B) or NPI52 (C and D) at 2 or 4 days post virus infection. Virus titers are expressed as $\log_{10} TCID_{50}$ per gram of liver tissue. Bar graphs show the fold reduction of geometric mean of virus titers in treatment groups compared to the control. Asterisks indicate significant differences between the control and the treated group ($* p < 0.05$, $**p < 0.01$).

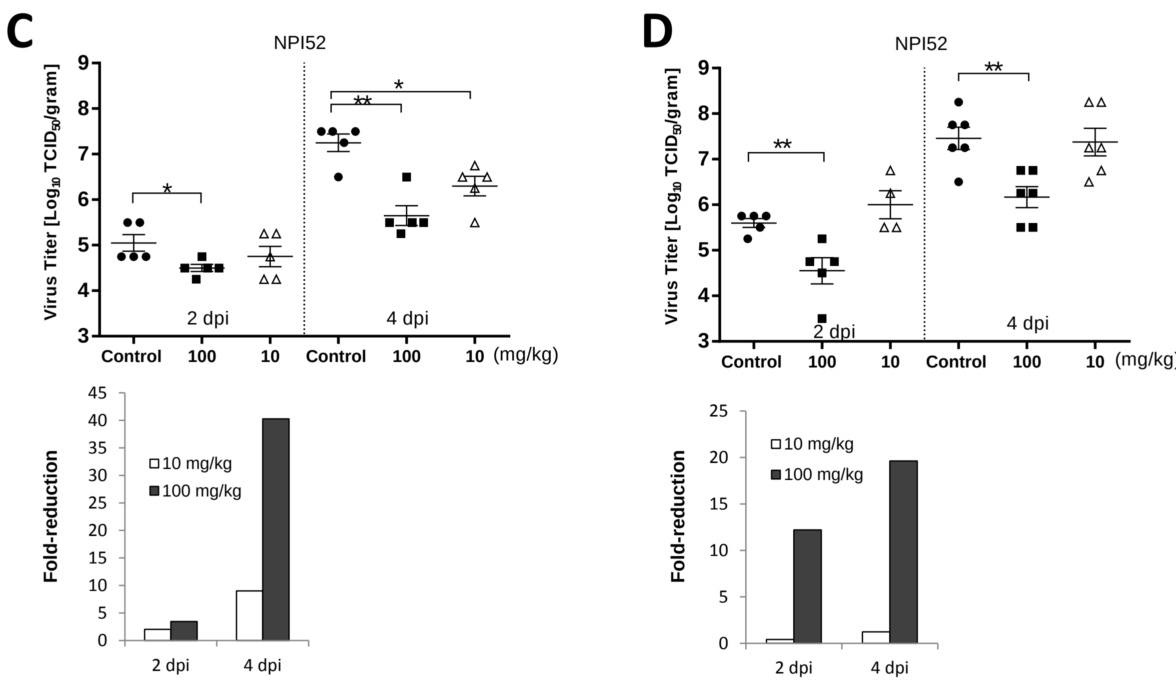

Figure 4. Effects of 3CLpro inhibitor treatment on MHV-A59 titers. Four to five week-old BALB/c mice were intraperitoneally inoculated with MHV-A59 at 5.2×10^5 (A) or 7.2×10^4 (B-D) $TCID_{50}$/mouse and treated with drug vehicle, GC376 (10, 50 or 100 mg/kg/day) or NPI52 (10 or 100 mg/kg/day) divided into two doses per day starting at 4 h prior to virus infection. Scatter plots show mean and the standard error of the means of virus titers in the liver of mice received mock (drug vehicle), GC376 (A and B) or NPI52 (C and D) at 2 or 4 days post virus infection. Virus titers are expressed as $\log_{10} TCID_{50}$ per gram of liver tissue. Bar graphs show the fold reduction of geometric mean of virus titers in treatment groups compared to the control. Asterisks indicate significant differences between the control and the treated group (* $p < 0.05$, ** $p < 0.01$).

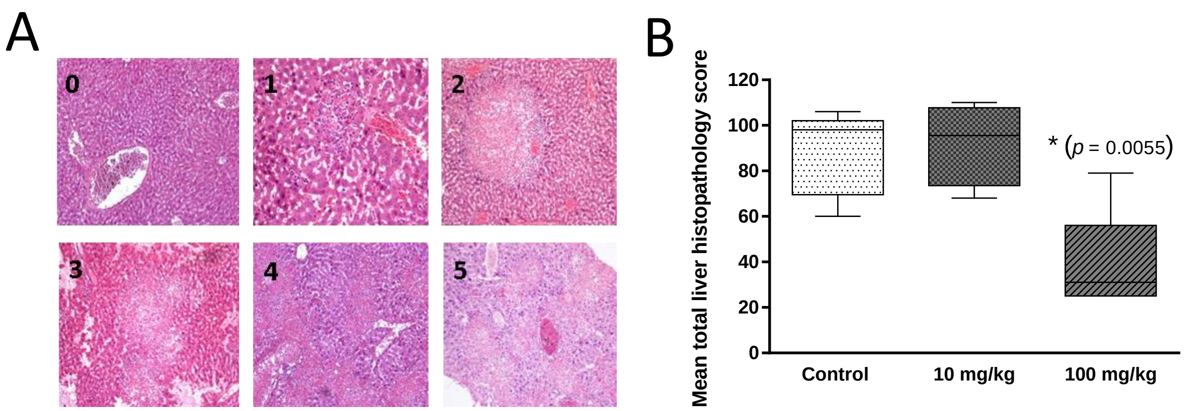

Figure 5. Histopathology changes in the liver of mice treated with NPI52. (A) Panels representing scores 0 through 5 with increasing severity of microscopic lesions. Score 0, minimal change; scores 1-2, multifocal areas of necrosis; and scores 3-5, coalescing areas of necrosis. (B) A box and whisker plot showing the mean total liver histopathology score for each group. (C) A table showing the frequency of histopathology scores in four (NPI52 10mg/kg) or five (control and NPI52 100mg/kg) liver samples per group. (D) A box and whisker plots showing the mean number of lesions per mouse liver for each group. Asterisks indicate statistically significant differences between control and NPI52 100 mg/kg-treated mice ($p < 0.05$). The whiskers represent 5% and 95% confidence intervals and the boxes represent 25% and 75% confidence intervals. The middle lines represent the median of the data.

Journal of Virology

C

	Frequency of lesions (%)		
Score	**Control**	**10 mg/kg**	**100 mg/kg**
1	29.1	35.6	30.8
2	23.2	35.6	57.9
3	32.4	28.8	11.2
4	10.3	0	0
5	4.9	0	0

D

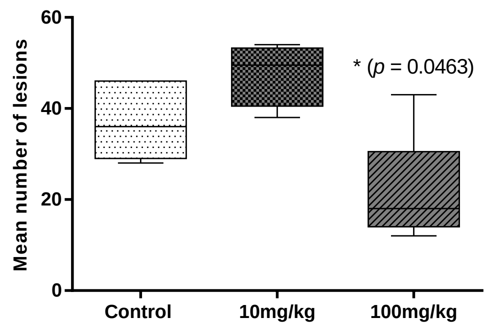

Figure 5. Histopathology changes in the liver of mice treated with NPI52. (A) Panels representing scores 0 through 5 with increasing severity of microscopic lesions. Score 0, minimal change; scores 1-2, multifocal areas of necrosis; and scores 3-5, coalescing areas of necrosis. (B) A box and whisker plot showing the mean total liver histopathology score for each group. (C) A table showing the frequency of histopathology scores in four (NPI52 10mg/kg) or five (control and NPI52 100mg/kg) liver samples per group. (D) A box and whisker plots showing the mean number of lesions per mouse liver for each group. Asterisks indicate statistically significant differences between control and NPI52 100 mg/kg-treated mice ($p < 0.05$). The whiskers represent 5% and 95% confidence intervals and the boxes represent 25% and 75% confidence intervals. The middle lines represent the median of the data.